Rates of Dissolution of Salt Minerals during Leaching Caverns in Salt—Fundamentals and Practical Application

Hans Ulrich Röhr

Deutsche Texaco A.G., P.O. Box 600849, 2000 Hamburg 60, Federal Republic of Germany

ABSTRACT

The rate of dissolution was calculated by means of formulas of Durie[1]. Using a corrective factor, satisfactory results were obtained for the rate of dissolution of halite. These formulas were used for calculating the rate of dissolution of other salts such as sylvinite, bischofite, kieserite, arcanite, glauber salt, carnallite and kainite. In the case of sylvinite and carnallite, the calculated rates of dissolution were relatively well in line with the results of laboratory test conducted by Hoffmann[7] With ternary or quarternary systems using NaCl, the maximum concentration of the diffusing mineral in the boundary is lower than with systems not using NaCl. It was assumed that a solubility equilibrium is reached in the boundary without the displacement of NaCl. Only with high NaCl concentrations, is NaCl displaced from the boundary. So far no details are available about the new equilibrium.

The computed rates of dissolution of different salts were related to the rate of dissolution of NaCl and the resulting relative rate of dissolution proved to be a suitable basis for planning. When leaching caverns, the selective dissolution should be reached. The leaching program is determined on the basis of a solution velocity diagram. Measures to be taken to reduce the NaCl concentration and the required control measures are described.

The selective dissolution after termination of the leaching process causes the formation of traps and possibly also jumps in the magnesium content. The relative rate of dissolution can be utilized for the recovery of potassium and magnesium salts.

INTRODUCTION

When caverns are leached in inhomogeneous salt, as occurs in Zechstein sequences, the different rates of dissolution of individual salt minerals result in irregular shapes of the caverns. This fact must be taken into account when planning and carrying out the leaching process and operation of the storage facility. For rock-mechanics reasons, an irregular cavern shape may cause breakdown of larger parts of rock. As a result, casings may be damaged or cut off and the access to lower parts of the cavern may be barred so that they cannot be used for storage purposes. Liquid storage products may be trapped in fingers leached in the upper part of the cavern so that they cannot be withdrawn again. With an irregular cavern shape, the salt body is not fully utilized, the storage capacity to be obtained per well is reduced and losses are increased during salt recovery. The irregularities of shape must also be taken into account when planning the withdrawal and reinjection processes.

Experience has shown that caverns can also be leached and utilized in salt of inhomogeneous composition. Knowledge of the factors influencing the shape of the cavern and particularly of the rate of dissolution of the individual salt minerals is required for this purpose. This paper is a contribution in this direction.

FUNDAMENTALS

Durie used an equation to express the width of the boundary layer for the binary system NaCl-H_2O. This equation is given as formula (1).

$$\delta_i = \frac{3.93}{(g \cdot \beta_i \cdot c_{si})^{1/4}} \cdot (D_i \cdot \nu_i \cdot x)^{1/4} \quad (cm) \qquad (1)$$

Where $\beta_i \cdot c_{si}$ is the maximum difference in density in the boundary layer, i.e. the difference in density between the saturated brine at the surface of the salt and the solution in the cavern. The meaning of the symbols used in the equations can be seen from the table at the end of the paper.

$$\beta_i \cdot c_{si} = \beta_{NaCl} \cdot (c_{NaCl_{max}} - c_{NaCl}) = \rho_{max} - \rho_{Sole} \ (g/cm^3) \quad (2)$$

If according to Durie[1], a parabolic concentration distribution from the vertical salt surface into the cavern is assumed,

$$c = c_{si} \cdot \left(1 - \frac{y}{\delta}\right)^2 \ (mol/l) \qquad (3)$$

the rate of dissolution as a function of diffusion can be expressed on the basis of Fick's law of diffusion by means of formula (4):

$$\left(\frac{dQ}{dt}\right)_x = \frac{2 \cdot K_i \cdot D_i \cdot c_{si}}{\delta_i \cdot \rho_k} \ (cm/s) \qquad (4)$$

Using (1) and (4), formula (5) was obtained by Durie by integrating over x-coordinate and taking the mean over height H

$$\frac{dQ}{dt} = 3.7975 \cdot \frac{K_i \cdot D_i^{3/4} \cdot c_{si}}{\nu_i^{1/4} \cdot H^{1/4} \cdot \rho_k} \cdot (\rho_{max} - \rho_{Sole})^{1/4} \ (cm/s) \quad (5)$$

Using (5) and (2), one gets formula (6) expressing the rate of dissolution for binary systems. (H = 1 cm)

$$\frac{dQ}{dt} = 3.7975 \cdot \frac{K_i \cdot D_i^{3/4} \cdot \beta_i^{1/4}}{\nu_i^{1/4} \cdot \rho_k} \cdot c_{si}^{5/4} = A_i \cdot c_{si}^{5/4} \ (cm/s) \qquad (6)$$

The author made an attempt to compute the rate of dissolution of different other salts[8], known as being diffusion-dependent, by means of formula (6), where binary salt-water systems at a temperature of 20°C were assumed.

For different salts Table 1 shows the constants D_i, C_{max}, ν_i, ρ_{max} according to[2] and ρ_k according to[2], the constants A_i and the maximum rate of dissolution according to formula (6) with $c_{si} = c_{max}$. With increasing salt concentration of the brine c_i, according to formula (6) c_{si} and, hence, the rate of dissolution decreases to a minimum value of zero (Fig. 1).

Durie[1] found that in the case of NaCl solutions the measurable rate of dissolution is increased by surface irregularities as against the computed values. It should be noted that the rate of dissolution computed for KCl is relatively well in line with the results of laboratory tests conducted by Hoffmann[7].

When leaching caverns in rock salt with seams or intercalations of other mineral salts, different rates of dissolution occur simultaneously due to the changing composition of the boundary. If over a large area a mineral other than halite is present at the cavern wall, the composition of the boundary is determined by this mineral. With low NaCl concentrations of the brine and low concentrations of the mineral present at the salt surface besides halite, only the concentra-

TABLE 1

Solution Values for Various Salts

	K_i	β_i	D_i	ν_i	ρ_{max}	ρ_K	c_{max}	A_i	$\frac{dQ}{dt}$	
	$\frac{g/cm}{mol/l}$	$\frac{g/cm^3}{mol/l}$	$10^{-5}cm^2/s$	cm^2/s	g/cm^3	g/cm^3	mol/l	10^{-4}	$10^{-3}g/cm^2s$	$10^{-5}cm/s$
Halite NaCl	0.05844	0.0368	1.40	0.013	1.1999	2.17	5.42	0.3035	0.545	0.251
Sylvinite KCl	0.07456	0.0432	1.81	0.0088 (0.0108)[1]	1.1742	1.984	4.03	0.5895 (0.5598)[1]	0.668	0.337
Kieserite $MgSO_4 \cdot H_2O$	0.13838	0.1061	0.51	0.0175 (0.0142)[1]	1.2961	2.57	2.79	0.344	0.319	0.124
Bischofite $MgCl_2 \cdot 6\ H_2O$	0.20322	0.0683	1.12	0.0137 (0.0134)[1]	1.3349	1.57	4.90	1.43 (1.43)[1]	1.628	1.037
Arcanite K_2SO_4	0.17427	0.1302	0.90	0.0103 (0.0115)[1]	1.0814	2.66	0.625	0.771	0.114	0.043
Glauber Salt $Na_2SO_4 \cdot 10H_2O$	0.32204	0.1164	0.77	0.014 (0.0133)[1]	1.1513	1.464	1.3	2.073 (2.0975)[1]	0.421	0.287

[1] Values for NaCl-bearing solutions

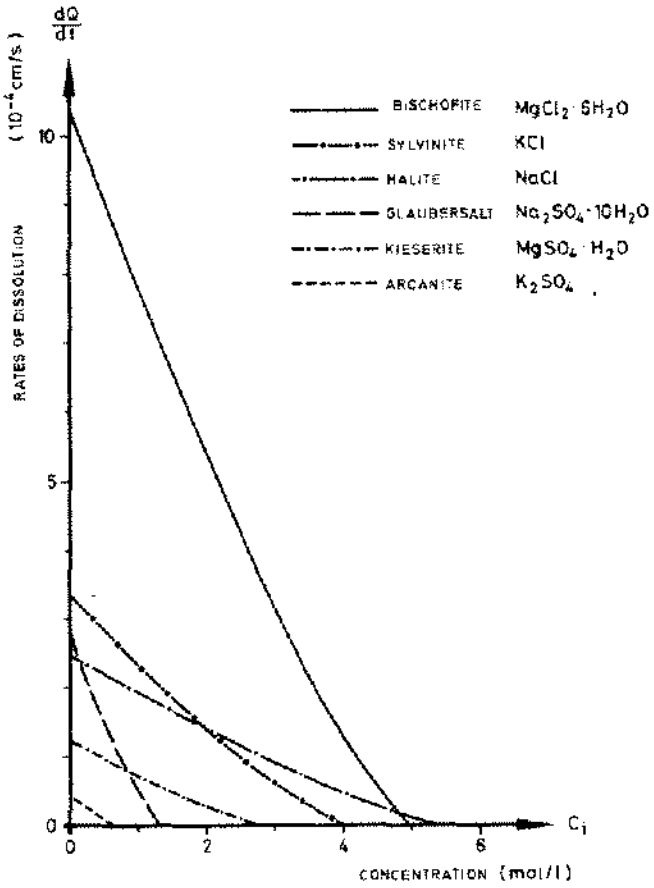

Figure 1. Computed rates of dissolution of binary salt-water systems depending on salt concentration at 20°C.

tion of this mineral will reach saturation c_{max} in the boundary. The maximum rates of dissolution were computed in Table 1.

With higher NaCl concentrations of the brine, the mineral present besides halite cannot reach saturation c_{max} in the boundary, as would have been the case in the binary system with H_2O. Solubility equilibria are established. It is assumed that the NaCl concentration of the brine remains unchanged in the cavern as well as in the boundary, i.e. that the NaCl is not displaced by another mineral.

Figures 2 and 3 show the maximum concentrations of different minerals with a given NaCl concentration in the boundary. The equilibrium diagrams of $KCl-NaCl-H_2O$ for sylvinite, $MgCl_2-NaCl-H_2O$ for bischofite, $Na_2SO_4-NaCl-H_2O$ for glauber salt, $KCl-Na_2SO_4-NaCl-H_2O$ for arcanite, $MgSO_4-MgCl_2-Na_2SO_4-NaCl-H_2O$ for kieserite were taken from d'Ans[4], those of $MgCl_2-KCl-NaCl-H_2O$ for carnallite and $MgCl_2-MgSO_4-KCl-NaCl-H_2O$ for kainite from Autenrieth[5, 6]. The concentrations were converted into mol/l.

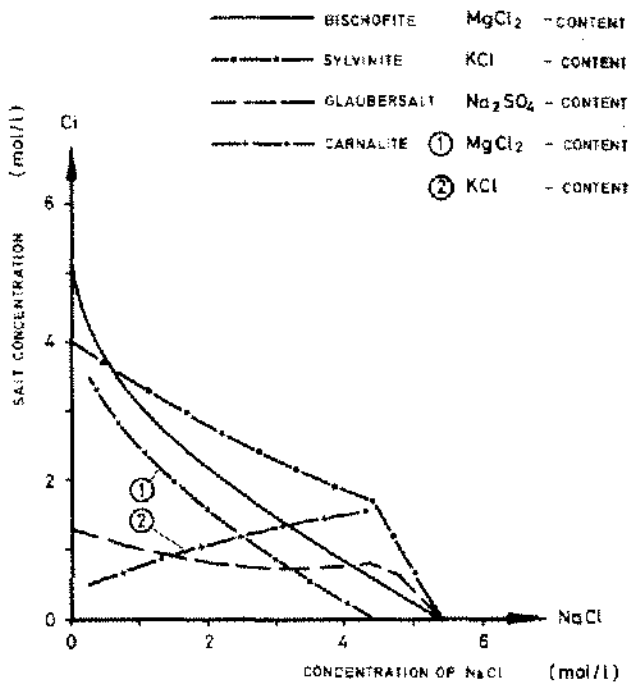

Figure 2. Equilibrium diagram with NaCl and H_2O at 20°C.

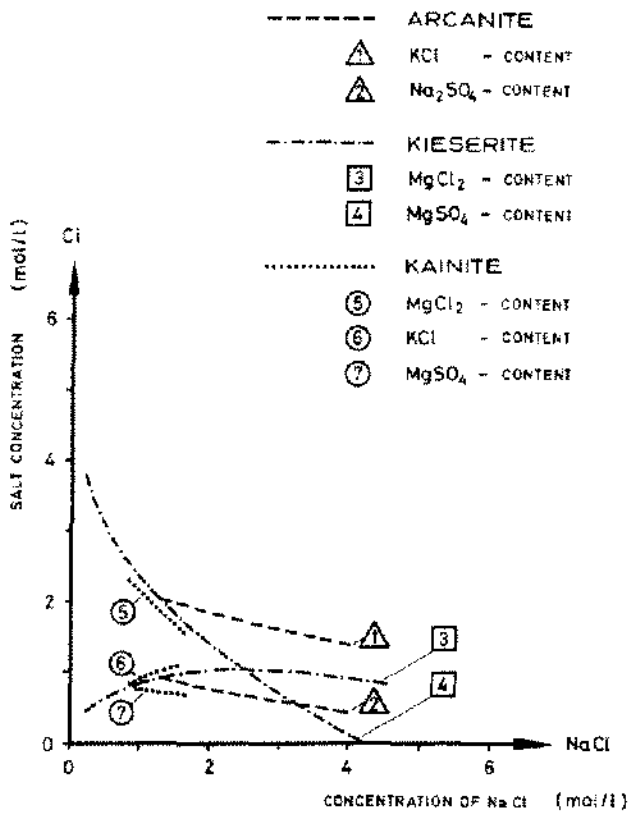

Figure 3. Equilibrium diagram with NaCl and H_2O at 20°C.

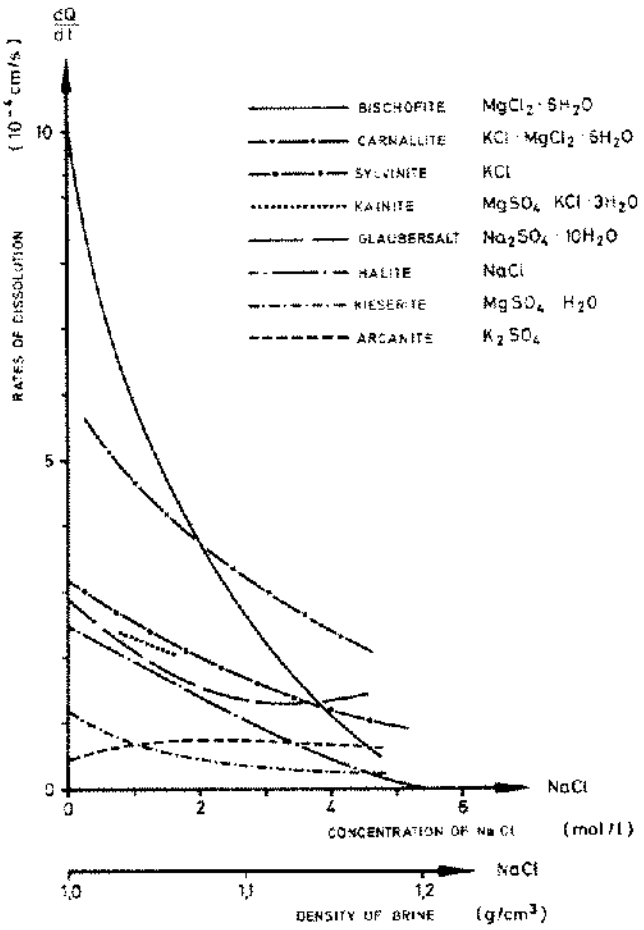

Figure 4. Computed rates of dissolution of ternary and quaternary salt-water systems at 20°C.

The rates of dissolution of sylvinite, bischofite, glauber salt in ternary systems with NaCl and H_2O were computed by means of formula (6). By taking the mean for viscosity (Table 1), slightly different values were obtained for A_i (Table 1). The maximum concentration of the mineral in the boundary (c_i in Figure 2) is to be equated with the concentration difference c_{si} in formula (6), if low concentrations of the mineral present at the cavern wall are assumed in the brine.

The density is expressed by the formulas (7).

$$\rho_{sole} = 1 + \beta_{NaCl} \cdot c_{NaCl}$$
$$\rho_{max} = 1 + \beta_{NaCl} \cdot c_{NaCl} + \beta_i \cdot c_i \qquad (7)$$

The rates of dissolution computed for KCl in NaCl solutions (Fig. 4) are relatively well in line with the values measured by Hoffmann[7]. The deviation increases with NaCl concentrations exceeding 4.5 mol/l. With high NaCl concentrations up to saturation, KCl continues to be dissolved, thus displacing NaCl in the boundary. Dissolution in an NaCl-saturated brine causes an NaCl undersaturation in the boundary. The rates of dissolution for nearly saturated NaCl solutions can therefore not be computed using the solubility diagrams (Fig. 2). The same applies to bischofite and carnallite dissolution.

Rate of dissolution of carnallite. As can be seen from Figure 2, carnallite ($KCl \cdot MgCl_2 \cdot 6\ H_2O$) decomposes and forms a quaternary system. With increasing NaCl concentration, the KCl content increases and the $MgCl_2$ content decreases. Laboratory tests conducted by Hoffmann[7] have shown that the rate of dissolution of carnallite uniformly decreases with increasing NaCl concentration. Comparable results are obtained by calculating the rate of dissolution of the KCl content and the $MgCl_2$ content by means of formula (5) and taking the arithmetic mean (Fig. 4), where

$$\rho_{max} - \rho_{Sole} = \beta_{KCl} \cdot c_{KCl} + \beta_{MgCl_2} \cdot c_{MgCl_2}$$
K_i = 0.27778
ρ_k = 1.6 g/cm³
ν_i = 0.0125 cm²/s
H = 1 cm

On the basis of the component with the lowest diffusion velocity, results would show a completely different trend than the laboratory results.

Rate of dissolution of kieserite. According to Figure 3, kieserite ($MgSO_4 \cdot H_2O$) decomposes and forms a quinary system with lower NaCl concentrations with an $MgCl_2$ and $MgSO_4$ content. With higher NaCl concentrations, $MgCl_2$ is replaced by Na_2SO_4. As in the case of carnallite, the rate of dissolution of the $MgCl_2$ content and the $MgSO_4$ content was calculated by means of formula (5) and by taking the mean (Fig. 4).

Rate of dissolution of kainite and arcanite. The dissolution of kainite ($MgSO_4 \cdot KCl \cdot 3\ H_2O$) results in a quinary system with an $MgCl_2$, a KCl and a $MgSO_4$ content (Fig. 3). The rate of dissolution of each content was calculated by means of formula (5) and taking the mean (Fig. 4).

There

$$\rho_{max} - \rho_{Sole} = \beta_{KCl} \cdot c_{KCl} + \beta_{MgCl_2} \cdot c_{MgSO_4} + \beta_{MgSO_4} \cdot c_{MgSO_4}$$
K_i = 0.24894
ρ_k = 2.15 g/cm³
ρ_{Sole} = 0.0137 cm²/s

Dissolution of arcanite (K_2SO_4) in NaCl solutions leads to a partial conversion to Na_2SO_4 and KCl (Fig. 3). The potassium diffuses as KCl and the sulfate as Na_2SO_4. The mean taken from the rate of dissolution of the Na_2SO_4 content and

TABLE 2

Relative Rate of Dissolution with 0 and 4.8 mol/l NaCl Concentration

C_{NaCl} (mol/l)	0	4.8
Halite	1	1
Kieserite	0.48	1.43
Arcanite	0.17	3.7
Bischofite	4.16	2.85
Sylvinite	1.28	5.7
Glauber salt	1.17	8.6
Carnallite	2.4	11.4
Kainite	1.08	5.5 extrapolated

the KCl content according to formula (5) can be seen from Figure 4.

Relative rate of dissolution. Special results are obtained by relating the calculated rate of dissolution of different minerals to the rate of dissolution of rock salt, taking into account the NaCl concentration of the brine (Table 2).

The relative solution velocity increases considerably with increasing NaCl concentration and causes selective dissolution of seams. The existence of kieserite-sylvinite seams is only indicated by their selective dissolution with an higher NaCl concentration, whereas carnallite seams are noticed even with minimum NaCl concentrations when surveying the cavity.

The solubility of different minerals has already thoroughly been investigated in the laboratory and described. Only little is known of the rate of dissolution and the underlying principles, however. The theoretical studies submitted in this paper is meant to be a contribution in this direction. Laboratory investigations of the solution velocity of as many different minerals as possible would be required in addition. Particularly the displacement velocity of selectively dissolving minerals in saturated NaCl lyes still has to be investigated. So far there do not exist any theoretical models describing this process.

PRACTICAL APPLICATION

Measures reducing selective dissolution. Detailed knowledge of the mineralogic and geological structure of the rock to be leached is required for taking the following steps:

1. Setting up a solution velocity diagram:

   Cores and log interpretations are used for detailed determination of the quantitative mineralogic composition. Assuming an average brine density (as it may occur during the leaching process later on) the relative rate of dissolution is determined for each depth interval by averaging the rates of dissolution of the respective mineral components. With flat-lying and axisymmetrically arranged rocks, the solution velocity diagram shows the development of the cavern as a nondimensional caliber and can thus be used as a basis for planning.

2. Planning the leaching program:

   The leaching steps can be determined on the basis of the solution velocity diagram. If possible, the individual steps should be chosen in such a way that a homogeneous selective rate of dissolution is ensured. Sections of great thickness with a high relative rate of dissolution should be leached in steps to keep the brine concentration down. Seams of low thickness with a higher relative rate of dissolution should be leached at the top of a leaching step. Selective dissolution can be reduced by injecting a blanket into the resulting traps. The maximum volume to be leached per step is reached when the maximum diameter to be obtained in horizontal direction under the given rock mechanical conditions is reached by the most readily soluble seam. With horizontal stratification and an axisymmetrical shape of the cavern, the relative rate of dissolution averaged over the depth interval is to the maximum relative rate of dissolution as the mean cavern diameter is to the maximum one. The rate of dissolution increases with the increasing dip and axially asymmetrical shapes are to be expected. The mean cavern diameter to be reached per leaching step must therefore be reduced by a factor.

3. Reduction of the NaCl concentration:

   On principle, the normal direction of circulation should be chosen, i.e. fresh water is pumped into the lower part of the cavern and the brine is withdrawn from the upper part.

   The highest circulation rates permitted by the leaching equipment should be chosen.

   The effective final volume to be leached per step should be relatively small with a correspondingly small surface.

   The leaching distance per step, i.e. the distance between the casing shoes of the leaching string and the protective string should be chosen as short as possible.

   The individual leaching steps should slightly overlap, since errors in depth cannot be entirely excluded when surveying the cavity and installing the casings. Furthermore, it must be ensured that the lower parts remain accessible for casings and equipment. Deviation of the well should on no account exceed 1.5 degrees. The above measures may also result in a reduction of the brine temperature and, hence, in a reduction of the selective rate of dissolution.

4. Intensive control of the leaching process may involve the following problems:

   Only the walls of the well are known. Any extrapolation for the adjacent areas may be wrong.

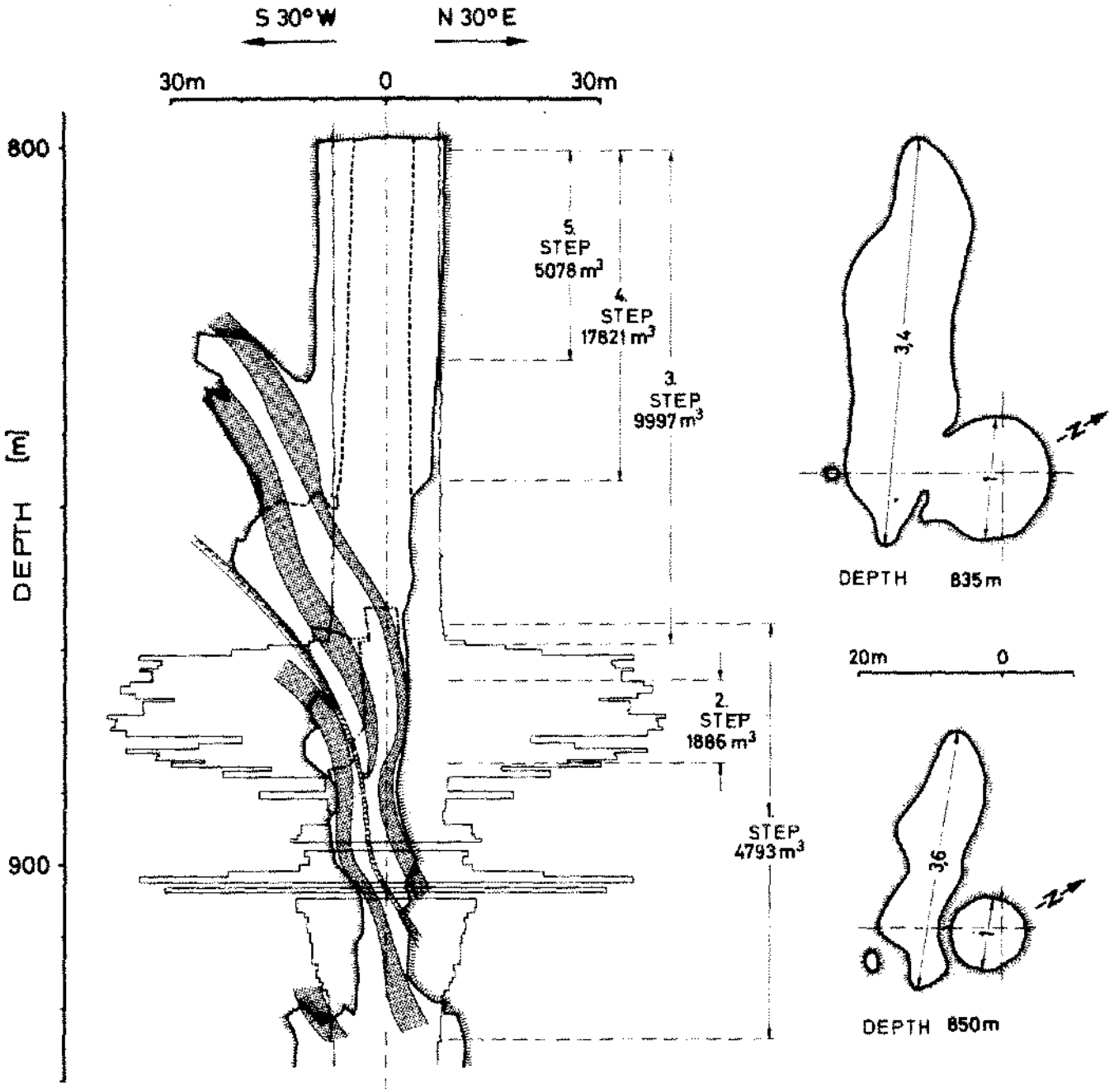

Figure 5. Development of the cavern shape. Vertical and horizontal cross section of a cavern with carnallite seams. Solution velocity diagram and leaching steps.

The mineralogic composition of the rock may change along the strike.

Seams at a small distance from the well may not be discovered by well logging due to the restricted depth of penetration of the measurements.

The dip stated in the well can only be assumed to be constant over a limited area.

Attention must therefore be paid to any indication of selective dissolution of a seam. Control includes continuous determination of the K and Mg contents as well as of the composition of the entire brine at longer intervals. The volume resulting from selective dissolution of the seam can thus be calculated at any time by means of these data. The increase in surface caused by selective dissolution leads to higher density values. The greater the deviation from the calculated values, the greater the extent of selective dissolution. The latter can also be controlled by determining the ratios KCl content/NaCl content, $MgCl_2$ content/NaCl content and $MgSO_4$ content/NaCl content of the brine.

Figure 5 shows a vertical section of a carnallite seam passing through the Sottorf 107 cavern with the solution velocity diagram and development of the cavern shape. At depths ranging from 869 to 888 m, the average mineralogic composition encountered in the well was as follows:

Carnallite	53,8%
Halite	40,2%
Kieserite	2,2%
Shale and anhydrite	3,8%

The seam was leached in five smaller steps (Table 3). Related to halite, the largest amounts of carnallite and kieserite were dissolved in the second step. The leaching distance exactly extended over the passing seam. With the low NaCl concentration, the relative rate of dissolution of carnallite was relatively low. With the medium NaCl concentration of about 3 mol/l, the relative rate of dissolution of carnallite, related to halite, was 3.4 (see Fig. 4). Leaching the 5th step was discontinued when determination of the solution velocity factor, the K and Mg contents indicated that the seam was leached again where the diameter was not to be increased any more.

The solution velocity factor A was calculated using formula (8) in accordance with the differential equations (25, 26, 27) described by Röhr[9].

$$A = \frac{Q_h \cdot c'}{(1.7 + 9.64 \cdot [0.147 - c']) \cdot (0.147 - c')^{1.25} \cdot S^{0.25} \cdot V_{Wirk}^{0.5}} \quad (8)$$

The solution velocity factor is directly proportional to the rate of dissolution of halite and the ratio surface of the cavity to surface of a cylinder of the same volume.

The relative rate of dissolution can be determined by relating the maximum diameter measured in horizontal direction at the depth where the seam is met by the well to the diameter simultaneously obtained in pure rock salt. The ratio can also be determined from a vertical section of the cavity in the direction of the seam dip (Fig. 6). The extent of the traps which have formed with known concentrations of the brine are thus an indication of the mineralogic composition of the seam.

The mineralogic composition of the seams encountered in the well at different depths was as follows:

		870 m	880 m	890 m
Halite	(Vol. %)	71.6	74.4	64.0
Sylvinite	(Vol. %)	5.2	3.5	1.3
Kieserite	(Vol. %)	12.3	12.1	11.4
Carnallite	(Vol. %)	—	—	18.1
Shale	(Vol. %)	2.2	3.9	5.2
Anhydrite	(Vol. %)	8.7	6.1	—

Attention must be paid to the fact that the traps increase in size due to the increase of the medium NaCl concentration from 3.9 mol/l to 4.75 mol/l.

Selective dissolution after termination of the leaching process. Laboratory measurements as well as measurements of the potassium and magnesium contents in completed caverns have shown that magnesium and potassium salts continue to be dissolved even in fully saturated NaCl solutions. Months after termination of the leaching process, the location of the casing shoe can still be seen from temperature jumps as well as from jumps in the magnesium

TABLE 3

Leaching Steps, Sottorf 107 Cavern

Step	Leaching Distance (m)	Water Flow (1000m³)	Dissolution Carnallite (m³)	Kieserite (m³)	Halite (m³)	A	Medium NaCl Concentration (mol/l)
1	57.8	62.5	500	100	4793	1.0	2.8
2	11.6	40.1	320	40	1886	0.5	1.7
3	68.8	128.5	1155	305	9997	0.7	2.9
4	46.2	181.3	1335	840	17821	1.4	3.6
5	29.5	78.3	1095	150	5078	1.9	2.4

content of the brine. This is due to the fact that parts of the brine with a slightly higher specific gravity are to be found further down and do not mix. Where mixing takes place, temperature jumps and jumps in the magnesium content are soon eliminated. Mixing may be caused by ascending lighter lyes rich in potassium.

When filling the storage cavern, the jumps in the magnesium content were used to predict the maximum storage capacity so that additional level controls were not required (Fig. 7). This can be illustrated by means of the following example. According to a sonar log, the storage capacity of a cavern located between 700 and 860.7 m was 123,500 m^3. In fact, 214,500 m^3 could be injected, however. The volume distribution over the depth range could be determined by means of sonic logs, 3 level controls and by stating 3 jumps in the magnesium content of the brine displaced during injection. The first injection of 24,400 m^3 to a depth of 730.8 m had been required for the last step of the leaching process. Temperature measurements carried out after termination of the leaching process revealed several temperature jumps indicating the oil level at a depth of 730.8 m and the location of the casing shoes during the respective leaching steps (792.5 m; 804 m; 836.5 m). In the course of further injection, three sudden decreases in the magnesium content were stated in the brine displaced from the cavern.

The volume measured between two jumps can be correlated with a depth range known from the leaching process. It was stated that the jumps in the magnesium content occurred at the same depth as the temperature jumps. After injection of another 40,000 m^3, i.e. of a total of 64,400 m^3, the first decrease was stated in the magnesium content, which was to be correlated with a depth of 836.5 m. During the initial injection already, the storage capacity available below 836.5 m thus proved to be 40,000 m^3 instead of the 27,000 m^3 expected according to the sonic log. The greatest deviation was stated between 730.8 and 792.5 m, where a

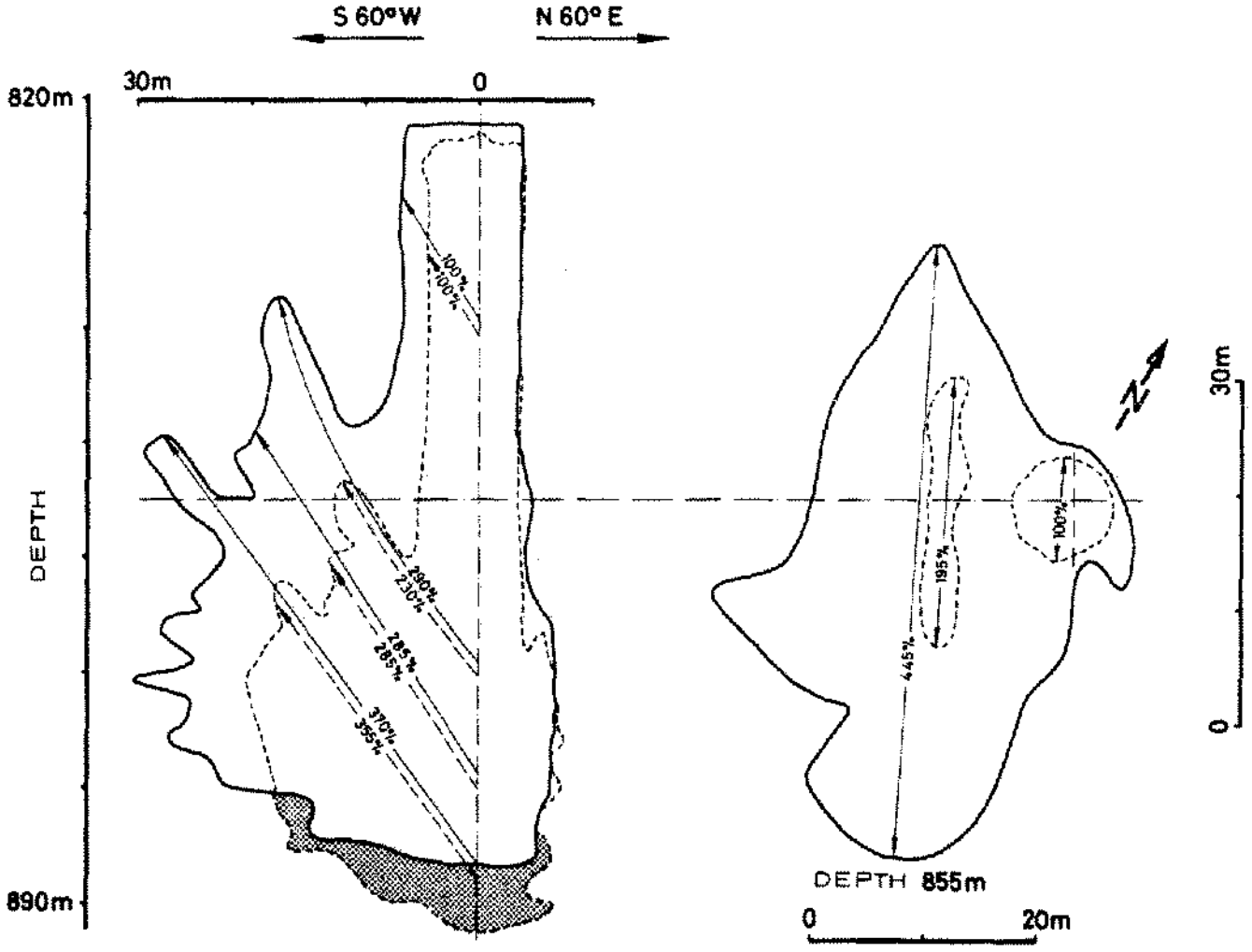

Figure 6. Selective dissolution of seams. Cross section in vertical and horizontal direction.

larger cavern section could be filled which had not been indicated by the sonic log. The storage capacity calculated from the volume of the dissolved salt proved to be relatively correct, however. It only deviated by a few percent from the cavern volume which could be filled.

Table 4 shows the increase in the magnesium content in the cavern at different depth ranges after termination of the leaching process.

If the increase in magnesium content is attributed to the dissolution of kieserte only, the volume is increased by 1.4 to 3,9 m^3/day where seams are present at the cavern wall. The seams have a kieserite-sylvinite facies, however, so that the volume is still increased by the dissolution of sylvinite.

In the course of the years, the traps are enlarged as a result of gradual dissolution of the seams, which are not indicated by a sonar log due to their small thickness. Selective dissolution could only be stopped after termination of the leaching process by filling the cavern with hydrocarbons.

NaCl saturation is reached after a few weeks, whereas potassium and magnesium salts still continue to be dis-

TABLE 4

Increases in Magnesium Content at Different Depths

Depth Range (m)	Brine Volume ($1000m^3$)	Period of Time (days)	Increase in Magnesium Content from: (g/l)	to: (g/l)	Dissolution of Magnesium (g/l day)	(t/day)	Kieserite (m^3/day)
836.5–865	40	290	1.8	14.6	0.044	1.77	3.9
804 –836.5	33	185	2.1	8.2	0.033	1.09	2.4
792.9–804	20	135	1.8	6.1	0.032	0.63	1.4

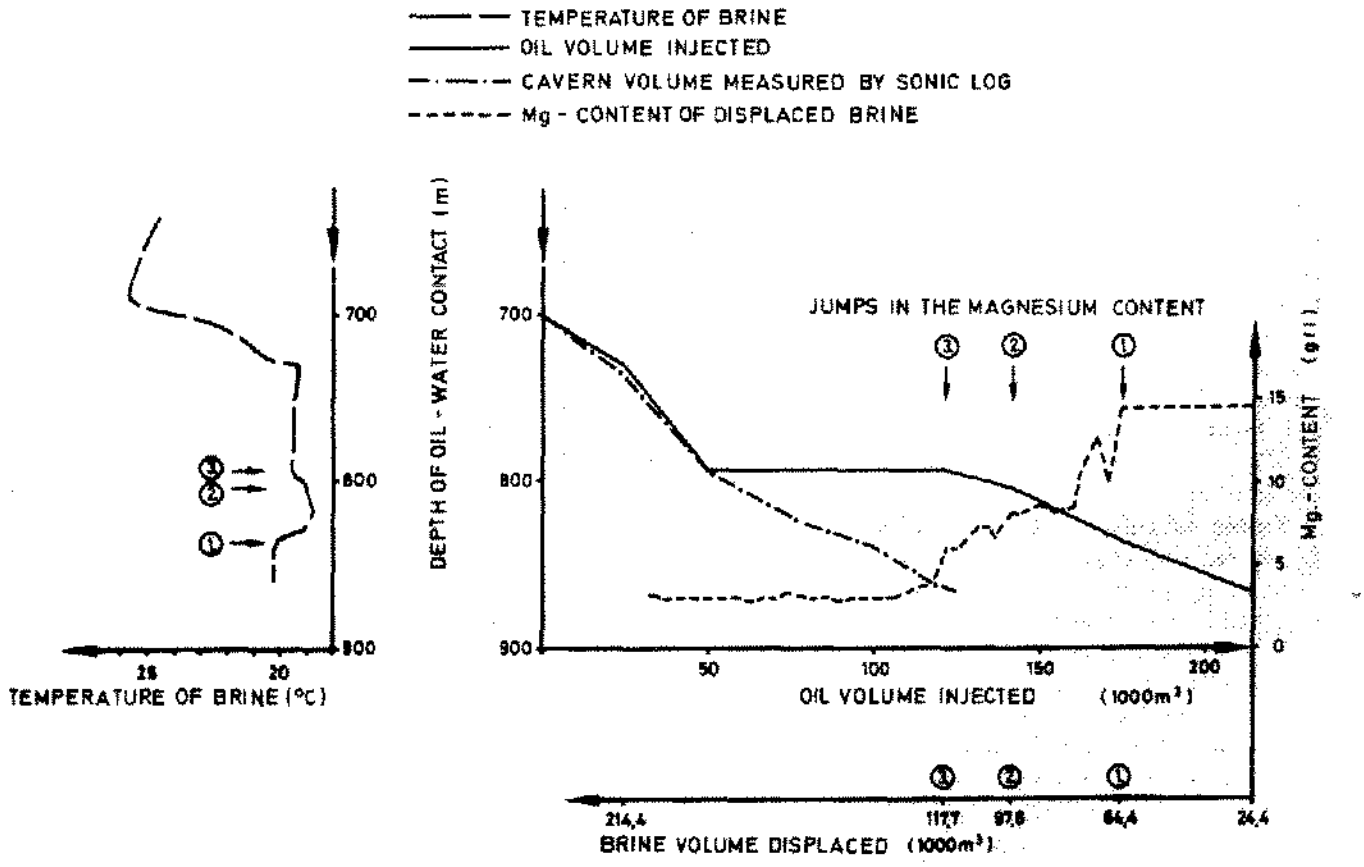

Figure 7. Oil volume injected and cavern volume by sonic log depending on oil-water contact. Content of Mg depends on brine volume displaced.

TABLE 5

Selective Dissolution Values with Time

Time after termination of the leaching process (days)		0	53	116	202	1026
Density by 20°C (kg/l)		1.172	1.204	1.211	1.216	1.240
Chloride	(m val/l)	4738	5602	5590	5638	5653
Sulfate	(m val/l)	43	51	164	187	496
Calcium	(m val/l)	24	28	46	34	12
Magnesium	(m val/l)	139	101	473	584	2101
Potassium	(m val/l)	62	165	172	177	192
Sodium	(m val/l)	4556	5359	5063	5030	3844
NaCl	(m val/l)	4556	5359	5063	5030	3844
KCl	(m val/l)	62	165	172	177	192
$MgCl_2$	(m val/l)	120	78	355	431	1617
$MgSO_4$	(m val/l)	19	23	118	153	484
$CaSO_4$	(m val/l)	24	28	46	34	12

solved for years after termination of the leaching process. The course of selective dissolution in the Sottorf 105 cavern is shown by Table 5 and Figure 8.

The depth range 710–720 m was investigated. The brine volume in this depth range was 72,000 m^3. The average mineralogic composition of the seam subject to selective dissolution was as follows:

Halite	76.3 Vol. %
Carnallite	12.0 Vol. %
Sylvinite	1.4 Vol. %
Kieserite	1.0 Vol. %
Shale	6.4 Vol. %
Anhydrite	3.0 Vol. %

After termination of the leaching process, the brine density first increased relatively quickly for 53 days. During this period full NaCl saturation was reached. The increase in brine density then slowed down.

Further selective dissolution of KCl and particularly of magnesium salts resulted in the displacement and precipitation of NaCl. As compared to the KCl content, the $MgCl_2$ and $MgSO_4$ contents increased relatively quickly. The $CaSO_4$ content first increased to a maximum value and then decreased again.

Taking advantage of the relative rate of dissolution for the recovery of potassium and magnesium salts. Sylvinite reservoirs of sufficient thickness and purity can be exploited by mining methods to a depth of approximately 1100 m. In deeper reservoirs and reservoirs where the concentrations are too low for exploitation by mining methods, recovery is possible by means of selective dissolution. An NaCl saturated brine is intermittently injected into the seam for this purpose. After a few months, the potassium salts will have displaced the sodium salts in the brine and a new solubility equilibrium will have formed. The brine rich in potassium will be displaced to surface from the cavity by

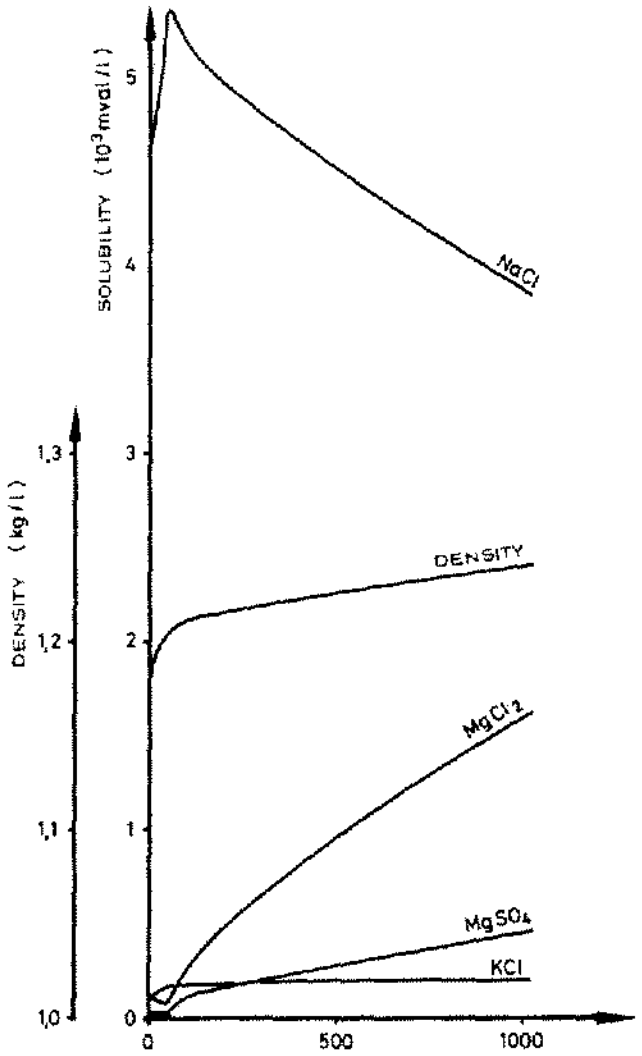

Figure 8. Selective dissolution of a carnallite seam after termination of the leaching process.

brine rich in sodium and cooling. The solubility of potassium chloride in water decreases to a higher degree at low temperatures than the solubility of sodium chloride.[4] Potassium chloride therefore precipitates and the potassium-deficient solution can be used again for selective dissolution. With a closed system using saturated NaCl brine the solution velocity of sylvinite is considerably lower than with a system using NaCl undersaturated brine, where NaCl dissolution takes place, but the solution velocity of KCl is also considerably higher. Furthermore, continuous operation is ensured. Before diluting the brine with water, a partial stream should be branched off.

Solutions with increased potassium or magnesium content in the brine are obtained by dissolution at higher temperatures. The solubility of sylvinite, bischofite and carnallite in NaCl solution increases more rapidly than the solubility of halite. Furthermore, the selective rate of dissolution of these minerals increases with respect to halite. This increase can be explained by the influence of the temperature on the diffusion constant, the viscosity and the solubility, as can be seen from formula (5). Increased brine temperatures are obtained naturally, if salt reservoirs at greater depths with higher reservoir temperatures are chosen.

DISCUSSION

Dr. Hans-Heinz Emons, Bergakademie Freiberg, German Democratic Republic.

Comment 1: Die Oberfläche beeinflußt aufgrund geometrischer, mineralogischer und chemischer Unterschiede maßgeblich die Lösungsgeschwindigkeiten, dieser Faktor muß bei genauen Berechnungen berücksichtigt werden.

Answer: Die Oberflächenregelmäßigkeiten vergrößern die meßbaren Auflösungsgeschwindigkeiten gegenüber den errechneten Werten. Das hatte bereits Durie für NaCl-Lösungen herausgefunden. Auf diesen Einfluß ist im vollständigen Text hingewiesen.

Comment 2: Beim Solen in carnallithaltigen Gesteinen ist der Einfluß des $MgCl_2$ entscheidender als der des NaCl auf die kinetischen Vorgänge, so daß $MgCl_2$ das bessere Bezugsmedium ist.

Answer: Bei führenden $MgCl_2$-Gehalten der Sole ist der $MgCl_2$-Gehalt mit Sicherheit entscheidender als der NaCl-Gehalt. Bei untergeordneten $MgCl_2$-Gehalten der Sole, aber hohen NaCl-Gehalten der Sole, wie sie beim Ausspülen bei Hohlräumen im allgemeinen auftreten, ist jedoch die relative Lösungsgeschwindigkeit bezogen auf die Lösungsgeschwindigkeit von NaCl eine sinnvolle Größe. Auch dazu wurden im Text ausführlichere Ausführungen gemacht, die in der kurzen Zeit, die für den Vortrag zur Verfügung stand, nicht im einzelnen dargestellt werden konnten.

REFERENCES

1. Durie, R.W. and Jessen, F.W. 1964. Mechanism of the Dissolution of Salt in the formation of Underground Salt Cavities. Society of Petroleum Engineers 4 (2) 183–190.
2. International Critical Tables of Numerical Data, Physics, Chemistry, and Technology, Vol. 3, London 1928.
3. D'Ans and Lax. 1967. Taschenbuch für Chemiker und Physiker, Springer Verlag, Berlin. Vol. 1.
4. D'Ans, J. 1933. Die Lösungsgleichgewichte der Systeme der Salze, ozeanischer Salzablagerungen, Kali-Forschungsanstalt, Berlin.
5. Autenrieth, H. Die stabilen und metastabilen Gleichgewichte des reziproken Salzpaares $K_2Cl_2 + MgSO_4 \rightleftharpoons K_2SO_4 + MgCl_2$ ohne und mit NaCl als Bodenkörper sowie ihre Anwendung in der Praxis, Kali und Steinsalz, Essen 1 (1952–55), Heft 7, S. 3–22.
6. ———, 1970. 50 Jahre deutsche Gemeinschaftsforschung auf dem Gebiet der Kalirohsalzverarbeitung. Kali und Steinsalz, Essen 1970, Heft 9, S. 289–306.
7. Hoffmann, H. 1969. Zur Lösungskinetik des Carnallits unter besonderer Berücksichtigung des Aussolprozesses von Mineralsalzlagerstätten, Bergakademie 21. Jahrgang 1969, Teil I, Heft 8, S. 486–490; Teil II, Heft 9, S. 554–558; Teil III, Heft 11, S. 674–678.
8. Sdanowski, A.B. 1958. Gesetzmäßigkeiten in der Kinetik der Salzauflösung. Freiberger Forschungshefte, A, 123: 257–268.
9. Röhr, H.U. 1969. Über die beim Spülen eines Untergrundspeichers in einem Salzstock wirksamen Einflußgeßgrößen im Hinblick auf die Gewinnung von Planungs- und Überwachungsunterlagen, Erdöl und Kohle–Erdgas–Petrochemie. 22: 670–679.

APPENDIX

List of Symbols.

A	Solution velocity factor	
A_i	Constant depending on the solution system	
C'	Salinity	(m^3/m^3)
c_i	Salinity of the brine	(mol/l)
c_{max}	Maximum Salinity	(mol/l)
c	Difference between water salinity at a point in the boundary and the salinity of the main body of water	(mol/l)
c_{si}	Maximum difference of salinity of the diffusing salt $c_{si} = c_{max} - c_i$	(mol/l)
D_i	Diffusivity constant	(cm^2/s)
g	Acceleration due to gravity = 981 cm/s^2	
H	Height of the vertical surface of the dissolving salt	(cm)
K_i	Conversion factor for conversion of the molar concentration (mol/l) into mass concentration using the crystal molar weight	
Q_h	Circulation rate	(m^3/h)

$\frac{dQ}{dt}$	Rate of dissolution	(cm/s)
S	Leaching distance	(m)
V_{wirk}	Effective volume of the cavity	(m^3)
X	Vertical direction	(cm)
Y	Horizontal direction from the wall into the cavern	(cm)
β_i	Conversion from concentration difference (mol/l) to the density difference (g/cm^3) $\beta_i = \frac{\rho_{max} - 1}{c_{max}}$	
δ_i	Width of the boundary layer	(cm)
ρ_{Sole}	Density of the brine in the cavern	(g/cm^3)
ρ_{max}	Maximum density of brine in the boundary	(g/cm^3)
ρ_K	Crystal density	(g/cm^3)
ν_i	Mean kinematic viscosity of the boundary	(cm^2/s)